Available online at www.sciencedirect.com
ScienceDirect
Geomorphology 81 (2006) 440–452
GEOMORPHOLOGY
www.elsevier.com/locate/geomorph

A comparison of methods used to estimate the height of sand dunes on Mars

M.C. Bourke [a,b,*], M. Balme [a], R.A. Beyer [c], K.K. Williams [d], J. Zimbelman [d]

[a] Planetary Science Institute, 1700 E. Ft. Lowell, Tucson, AZ 85719, USA
[b] Oxford University Centre for the Environment, University of Oxford, Oxford, OX1 3QY, UK
[c] NASA Ames Research Center, MS 245-3, Moffet Field, CA 94035, USA
[d] Center for Earth and Planetary Studies, National Air and Space Museum, Smithsonian Institution Washington, DC 20013, USA

Received 17 November 2005; received in revised form 21 April 2006; accepted 25 April 2006
Available online 7 July 2006

Abstract

The collection of morphometric data on small-scale landforms from other planetary bodies is difficult. We assess four methods that can be used to estimate the height of aeolian dunes on Mars. These are (1) stereography, (2) slip face length, (3) profiling photoclinometry, and (4) Mars Orbiter Laser Altimeter (MOLA). Results show that there is good agreement among the methods when conditions are ideal. However, limitations inherent to each method inhibited their accurate application to all sites. Collectively, these techniques provide data on a range of morphometric parameters, some of which were not previously available for dunes on Mars. They include dune height, width, length, surface area, volume, and longitudinal and transverse profiles. The utilization of these methods will facilitate a more accurate analysis of aeolian dunes on Mars and enable comparison with dunes on other planetary surfaces.

Keywords: Aeolian; Dune; Mars; Morphometry; Methods; Remote sensing; Planetary geology

1. Introduction

Morphometry is an important tool for understanding the evolution of landforms. It is the starting point for the explanation of geomorphological process and allows us to predict, empirically, a range of processes and dynamics (Whalley, 1990). This is particularly valuable in planetary geology, where it is often the only way in which these processes can be assessed. On Earth, geomorphologists often have direct access to landforms in the field and can collect data on overall size and shape-in some cases to centimeter accuracy (e.g., Nagihara et al., 2004; Stokes et al., 1999). On other planetary surfaces, the acquisition of similar high resolution data is severely constrained. Nonetheless, in recent years significant improvements have been made in the range of data that are being returned from Mars for use by geomorphologists. These include satellite data with spatial resolutions of up to 1.5 m/pixel (Malin and Edgett, 2001) and temporal resolution of months to years (Edgett et al., 2000). Laser altimetry has resulted in the production of a global topographic map (Smith et al., 1999), and a stereo camera (i.e., the HRSC on Mars

* Corresponding author. Planetary Science Institute, 1700 E. Ft. Lowell, Tucson, AZ 85719, USA.
E-mail addresses: mbourke@psi.edu (M.C. Bourke), mbalms@psi.edu (M. Balme), rbeyer@arc.nasa.gov (R.A. Beyer), williamskk@si.edu (K.K. Williams), zimbelmanj@si.edu (J. Zimbelman).

0169-555X/$ - see front matter © 2006 Elsevier B.V. All rights reserved.
doi:10.1016/j.geomorph.2006.04.023

Express) allows for the estimation of topography at a scale that is suited to geomorphic studies of medium-scale landforms (e.g., Jaumann et al., 2005). Thermal emission data allows estimation of grain size (i.e., dust and sand can be distinguished from bedrock, e.g., Zimbelman and Leshin, 1987); and recently, minerology and lithology can be detected at both global and local scale (e.g., Bandfield et al., 2000; Christensen et al., 2001, 2005; Wyatt and McSween, 2002).

These satellite data sets have enabled planetary geologists to analyse Martian aeolian dunes at a range of spatial scales. For example, a program to map the global distribution of Martian sand seas is underway (Hayward et al., 2004), and we can now begin to examine in detail the hypotheses for the evolution of sand seas in specific geological and topographic locations (e.g., Bourke et al., 2004b; Byrne and Murray, 2002; Edgett et al., 2003; Fenton et al., 2003; Fishbaugh and Head, 2005; Mullins et al., 2004; Thomas and Weitz, 1989). We currently have the capability to collect data on aeolian dune type, location, sediment size, lithology, and provenance and to search for evidence of dune migration (e.g., Anderson et al., 1999; Bourke et al., 2004a; Edgett and Christensen, 1991; Edgett, 2002; Garvin et al., 1999; Langevin et al., 2005; Williams et al., 2003; Zimbelman, 2000). We can use atmospheric models to predict wind regimes at decadal, seasonal, and even diurnal time-scales (e.g., Bourke et al., 2004b; Fenton and Richardson, 2001; Fenton et al., 2005; Haberle et al., 1999; Rafkin and Michaels, 2003; Toigo and Richardson, 2003). At a more local scale, the Lander and Rover data sets have made possible the detailed examination of small-scale aeolian dunes (centimetre to meter scale) and detection of aeolian grain size and mineral composition (e.g., Greeley et al., 1999, 2002, 2004; Sullivan et al., 2005).

The next challenge is to assess the dynamics and evolution of individual aeolian dunes under a Martian atmosphere, which today has a radically different composition, density, and temperature regime from that on Earth. On Earth, barchan dune form is known to be directly controlled by aerodynamic processes, whereby constant feedback occurs between the windward dune shape, slip face height, and horn-to-horn width (Hesp and Hastings, 1998). This allometric relationship between morphometric variables on dunes has been statistically established and used to relate dune size, shape, and form to wind regime and sediment supply (e.g., Finkel, 1959; Hastenrath, 1967; Mabbutt, 1977; Ewing, 2004; Hesp and Hastings, 1998; Lancaster, 1988). These relationships have not yet been established for dunes on Mars and the application of Earth-derived relationships may be erroneous. In addition, barchan planform shape on Mars is highly variable (see Fig. 1 in Bourke et al., 2004a) and in many cases it may be difficult to locate suitably shaped bedforms. Given the improved data currently being returned from Mars, we can now attempt to establish morphometric data sets and test if similar relationships exist (e.g., Bourke et al., 2003, 2004a).

High resolution Mars Orbiter Camera (MOC) images permit two-dimensional morphometric data to be collected with precision up to ~1 pixel (i.e., potentially as good as 1.5 m). Dune width, length, and surface area, for example, can all be estimated from these images. However, the estimation of dune height is more difficult. Mars Orbiter Laser Altimeter (MOLA) data average topography over a 100-m ellipse and have a shot spacing of ~300 m (Smith et al., 2001). This is suitable for the measurement of the large-scale surface topography, but many aeolian dunes are below this resolution. Prior to the beginning of the Mars Global Surveyor mission in 1997, a suite of methods were used to estimate the relative height of landforms on Mars. These methods include photoclinometry (e.g., Howard et al., 1982), shadow length (e.g., Arthur, 1979), and stereography (e.g., Parker and Schenk, 1995). Recently, a number of research teams have adopted and refined methods for estimating small-scale landform height (Beyer et al., 2003; Bourke et al., 2004a; Williams, 2003). In this paper we come together to compare these methods and apply them to aeolian dunes. This analysis is intended to test the robustness of the methods and to establish the advantages and relative limitations of each method.

2. Methods

We estimated the height of barchan dunes, barchanoid ridges, and transverse aeolian ridges (TARs) at seven locations on Mars (Figs. 1 and 2) and independently applied each method. In order to estimate maximum dune height, we selected a location at the highest point on the dune crest (when possible), usually interpreted as the top of the longest slip face in the MOC image. We attempted to apply all four methods to each sample location; however, this sample design was hampered by the inherent limitations of some of the techniques (e.g., availability of suitable MOLA sample shot locations).

2.1. Method 1, stereography

Dune height can be measured using overlapping Mars Orbiter Camera (MOC) narrow angle images

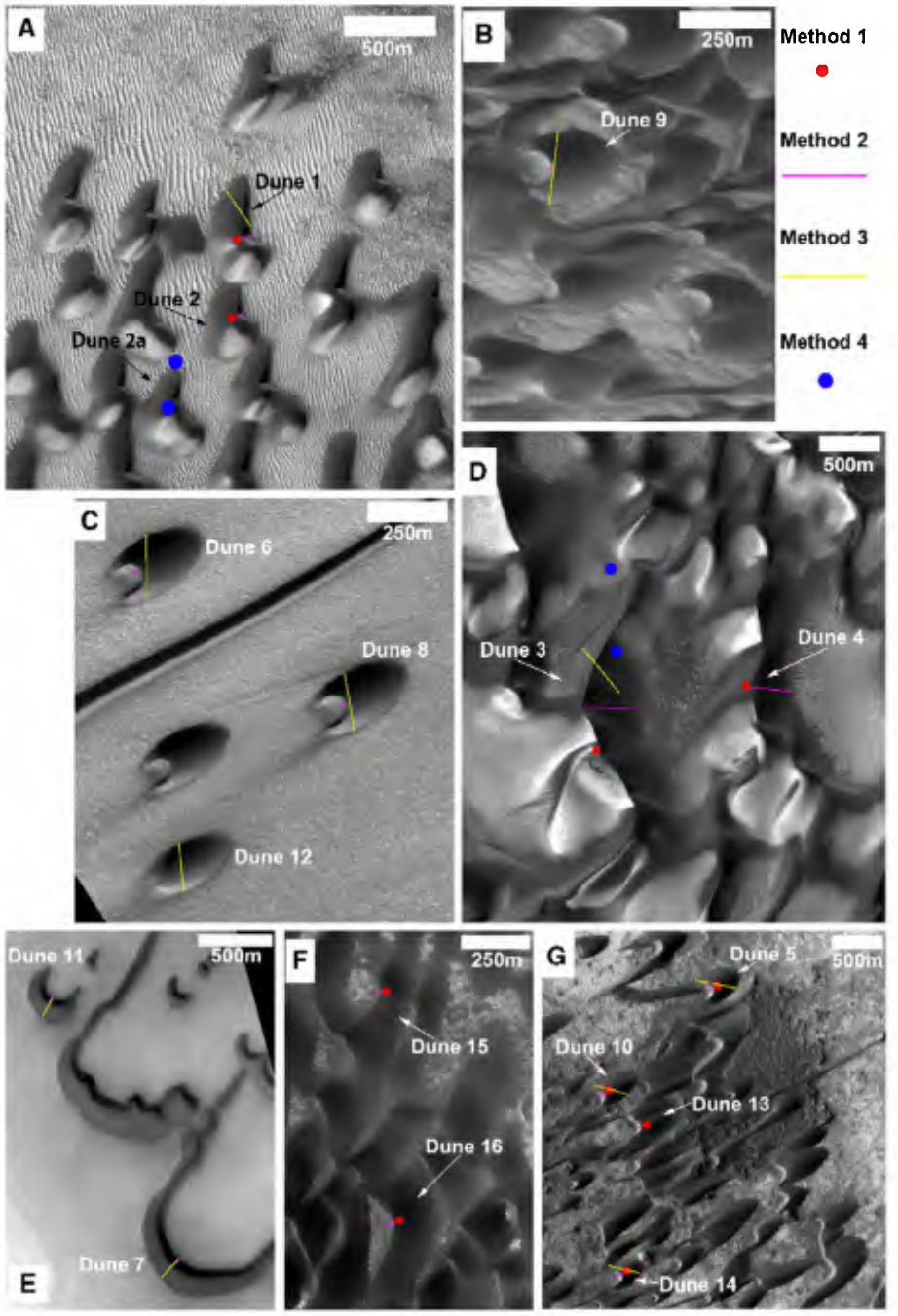

Fig. 1. Location of sample sites. The red dot indicates the location of the height estimate by the stereography method (method 1). The pink line, located down the slip face of the dune indicates the line of measurement for method 2. The yellow line indicates the location of the photoclinometric profile line (method 3). The blue dot is the location of the MOLA footprint (method 4). Every effort was made to coincide the location of the sample point or transect for each of the methods; however, this was often hampered by the restrictions of the method, e.g., the transect for method 3 (yellow line) had to be aligned with the Sun angle. (A) Proctor Crater, E03-01039, 4.87 m/px. (B) Chasma Boreale, E04-01496, 25.77° W., 84.96° N., 6.52 m/px. (C) Chasma Boreale, M19-01945, 26.66° W., 84.84° N., 4.85 m/px. (D) Proctor Crater, E03-01039, 4.87 m/px. (E) North Polar Sand Sea, M02-02835, 255.24° W., 8.66° N., 3.22, m/px. (F) Crater near Herschel Basin, M1102107, 232.01° W., 16.53° N., 2.82 m/px. (G) Syrtis Major Caldera, E03-02016, 232.01° W., 16.53° N., 2.82 m/px. See Table 1 for results.

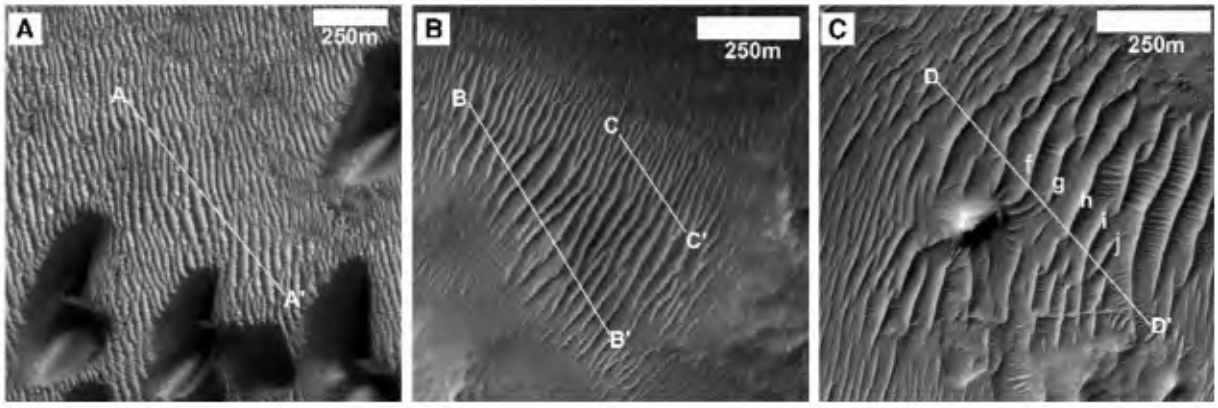

Fig. 2. Location of TAR sample sites. A) Transect A, Proctor Crater, E03-01039, 4.87 m/px. B) Transect B and C, in Gorgonum Chaos close to a Crater rim, M18-01072, 169.30° W., 37.57° S., 2.7 m/px. C) Transect D, Nirgal Vallis, M00-02226, 39.96° W., 28.71° S., 1.39 m/px. See Table 2 for results.

(Williams, 2003). Images from the nominal mission were acquired at near-nadir angles and extended mission images are off-nadir, thus giving stereo coverage in repeat-pass areas. In areas where a pair of images has sufficient resolution, adequate angular separation, and the correct orientation, dune heights can be calculated using the following method. First, both raw images are resampled to the correct aspect ratio and to 1 m/pixel spacing. Transects are then drawn across each image parallel to the viewing direction, such that they cross dune crests and distinct features such as boulders or outcrops. Along these transects, distances are measured between common points in each image (i.e., boulders, dune edges, and dune brinks). These measurements are then projected at the viewing angles of the images, creating a topographic profile across the transect. The difference between the measured dune brink and the dune base gives a geometric measurement of the dune height. This method has been used to establish the first height estimates of TARs on Mars (Williams and Zimbelman, 2003) and is being conducted in tandem with a search for dune migration and changes in dune form (Williams et al., 2003). We estimated the height of 10 dunes and two TAR trains on Mars using this method (Tables 1 and 2).

2.2. Method 2, slip face length

The length of the avalanche face of dunes, measured from high-resolution MOC images, can be used to estimate the height of dunes on Mars (Bourke et al., 2004a). This method is best suited to features where slip faces are clearly identified. Illumination effects often accentuate the lee slope, especially when the slip face is oriented orthogonal to the Sun, and frequently allow for a more accurate measurement. Most MOC images are near-nadir, so orthorectification is not needed before making length measurements. However, care must still be taken to account for pixel geometry. Dune and TAR heights are estimated by

Table 1
Dune height estimates

Dune	Stereography (1) (m)	Slip face length (2)[i] (m)	Profiling photoclinometry (3) (m)	MOLA (4) (m)
1	**33**	**32±5**	5–6[ii,iii]	
2	**30**	**22±5**		
2a		**25±5**		**22**
3	87	224–275±5[iii]	20[ii]	85[ii]
4	90	170–204[iii]		
5	**77**	**67±3**[iii]	**70**[ii]	
6		35±10[iii]	20–25[ii]	
7		27±2	10	
8		32±3[iii]	20[ii]	
9		**21±7**[iii]	**25**[ii]	
10	**61**	38±10	**50**[ii]	
11		19±2	5	
12			15	
13	**~25**	**23±2**		
14	**40**	**50±3**[iii]	**50**	
15	4.5[iii]	39±3		
16	32	88±3		

Values in bold indicate good agreement between methods.
[i]Measured at/from dune brink.
[ii]Not located at the highest point on the dune brink.
[iii]Data output during measurement indicate the result may be inaccurate.

Table 2
Height estimates of transverse aeolian ridges (TARs) on Mars

TAR transect	Method 1 min–max (m)	Method 2 (m) assume slope angle of 10°	Method 2 (m) assume slope angle of 25°	Method 2 (m) assume slope angle of 33°	Method 3 average (m)
A–A′	5.5–6		2.7–6.5	3.2–7.8	2–3
B–B′	2–6		1.8–5	2.2–6	2–3
C–C′			1.8	2.2	1–2
D, f		2.0±0.2	5.2±0.8	7.2±0.8	2
D, g		1.2±0.2	3.2±0.6	4.5±0.9	1
D, h		2.2±0.2	5.8±0.6	8.1±0.9	3
D, i		2.0±0.2	5.2±0.6	7.2±0.9	2
D, j		1.5±0.2	3.9±0.6	5.4±0.9	2
Small TARs (Fig. 4)					0.25

converting slip face length, assuming an angle of repose. The angle of repose for large dunes on Mars cannot be directly measured, but Greeley et al. (1999) found that the angle of repose at the Mars Pathfinder landing site is similar to that for sand on Earth (i.e., 33°). In addition, an angle of 32.4° was estimated from exposed stratigraphy observed in ground-based images of dune material at Ares Valles (RoverTeam, 1997, see their Table 1). In this study we therefore assume an angle of repose of 33°.

TARs have not yet been determined to be transverse dunes or mega-ripples (Wilson and Zimbelman, 2004). We use estimates of angles associated with ripple lee slopes as well as dune slip face slopes for the estimation of TAR height. On Earth, the lee slope of a ripple is composed of a short straight section near the crest at an angle of about 30–34° (Bagnold, 1941; Pye and Tsoar, 1990; Sharp, 1963) followed by a longer concave section. We use three average lee slopes of TARs at 10°, 25°, and 33°. The height of sixteen dunes and four TAR trains on Mars was estimated using this method (Figs. 1 and 2; Table 2).

2.3. Method 3, profiling photoclinometry

Photoclinometry (more descriptively, shape-from-shading) is a technique that uses brightness (radiance) information from an image to infer topography. Using point photoclinometry (Beyer et al., 2003), accurate upper limits to surface slopes can be made at the pixel scale. First, a profile is selected across the sample surface. This profile must be in the down-Sun direction, which may not always be parallel to the orientation of the appropriate landform transect (e.g., see Fig. 2A). A topographic profile can be created by finding the relative difference in elevation across each pixel. The topography is derived from the surface slope of pixels in a profile and the projected size of those pixels on the surface. The point photoclinometry method returns a slope for each pixel; and to convert that into a change in elevation across that pixel, the width of the pixel in distance units must be known, as well as the down-Sun direction. We make the simplifying assumption that the distance (d) across each pixel in the profile is identical, calculated as follows:

$$t = \begin{cases} \sin\alpha & \frac{\pi}{4} < \alpha < \frac{3\pi}{4} \quad \text{or} \quad \frac{5\pi}{4} < \alpha \frac{7\pi}{4} \\ \cos\alpha & \alpha < \frac{\pi}{4} \quad \text{or} \quad \frac{3\pi}{4} < \alpha < \frac{5\pi}{4} \quad \text{or} \quad a > \frac{7\pi}{4} \end{cases} \tag{1}$$

$$d = \frac{r}{|t|} \tag{2}$$

where r is the image resolution (or length of a pixel side) and α is the solar azimuth (relative to the horizontal axis of the image) in radians. Once the distance across each pixel, d, is obtained from the above equation, the elevation difference, δ_z, can be determined across each pixel. If a given pixel has a slope, θ, then $\delta_z = d\ tan\theta$. The distance across each pixel and the elevation difference across each pixel can be put together to make a topographic profile of elevation as a function of distance along that profile. This technique is suitable for Martian conditions where the underlying albedo is relatively constant at the small-scale, and an accurate estimation of the brightness of a flat surface can be made. We estimated the height of eleven dunes and five TAR trains on Mars using this method (Tables 1 and 2). Photoclinometry has also been applied to measure small gully forms on the Reiss crater dunes (Miyamoto et al., 2004) and MER landing site topography (Beyer et al., 2003).

2.4. Method 4, MOLA

MOLA acquired measurements of topography have an optimum vertical resolution of ~30 cm. The data consist of regularly spaced footprints, ranging in size from 70 to 150 m with a shot spacing of 330–390 m (Garvin et al., 1999; Smith et al., 1998). In some locations, two MOLA shots might coincide with the crest of the dune and the interdune or surrounding terrain (e.g., Fig. 1D). This is more likely for profiles over the larger dune masses. These MOLA data points can then be used to estimate the dune height. MOLA data have been used to estimate the average height of dunes in intracrater sand seas and the North Polar Sand Sea (e.g., Fenton et al., 2003; Garvin et al., 1999; Neumann, 2003). We estimated the height of two dunes on Mars using this method (Table 1). However, no TARs were sampled as the MOLA footprint was too large and frequently overlapped both the ridge and the swale.

2.5. Empirical methods

On Earth, barchan dune height is essentially one tenth that of its horn-to-horn width (see Hesp and Hastings, 1998). It is unknown if similar relationships exist for dunes on Mars. One way to test this is to compare dune height estimates on Mars with values estimated using empirical relationships established for dunes on Earth. We compare empirically derived estimates to those produced by method 2 (Table 3). We use Mabbutt's (1977) estimation of dune height at 10% of dune width. In addition, the following formulae were used:

$$h = w{-}5.75/9.58 \quad (3)$$

where h=dune height and w=horn to horn width (Finkel, 1959)

$$h = w{-}9.52/8.19 \quad (4)$$

(Hastenrath, 1967, 1987)

$$h = w{-}7.65/8.82 \quad (5)$$

(1, Hesp and Hastings, 1998)

$$h = w + 15.77/18.37 \quad (6)$$

(2, Hesp and Hastings, 1998)

3. Results

We have estimated the height of a total of 17 dunes (barchans and barchanoid) and 5 transects across TAR trains (Table 1 and 2). We consider that estimates that fall between a ratio of 0.7 and 1.3 to be 'in good agreement'.

3.1. Dunes

Several of the sample sites had good agreement between the different methods (these results are in bold in Table 1). There is good agreement between methods

Table 3
Empirical estimates of dune height of Mars using established relationships for Earth

Dune	Note	Width (m)	Finkel (1959)	Mabbutt (1977)	Hastenrath (1967, 1987)	Hesp and Hastings 1 (1998)	Hesp and Hastings 2 (1998)	Method 2
1	Asymmetric	311	31.9	31.1	36.8	34.5	17.8	32±5
2	Asymmetric	151.4	15.2	15.2	17.3	16.3	9.1	22±5
2a	Asymmetric	305.7	31.3	30.6	36.2	33.8	17.5	25±5
5	Strongly asymmetric	163	16.4	16.3	18.7	17.6	9.7	67±3
6	Ovoid barchan	94	9.2	9.4	10.3	9.8	5.9	35±10
6	As above	178*	18	17.8	20.6	19.3	10.5	as above
7	Limb extension	736.5	76.3	73.7	88.8	82.6	41	27±2
8	Ovoid barchan	90.5	8.9	9.1	9.9	9.4	5.8	32±3
8	As above	171*	17.25	17.1	19.7	18.5	10.1	as above
9	Barchan	183	18.5	18.3	21.1	19.8	10.8	21±7
10	Asymmetric	186	18.8	18.6	21.6	20.2	11	38±10
11	Barchan	232.6	23.7	23.3	27.2	25.5	13.5	19±2
13	Coalesced, asymmetric	251	25.6	25.1	29.5	27.6	14.5	23±2
14	Limb extension	170.2	17.2	17	19.6	18.4	10.1	50±3

Horn-to-hom width was used except where noted by * where maximum dune width was used. Dunes highlighted in bold have good agreement between methods in Table 1. Dunes in italics show good agreement between Method 2 and the empirical estimates.

1, 2, and 3 for dunes 5 and 14. There is also good agreement in the values produced by the slip face length (2) and stereography (1) methods for dunes 1, 2, 5, 13, and 14 and for dune 10 between methods 1 and 3. Methods 2 and 3 show similar results for dunes 5, 9, 10, and 14. The height of dune 2a estimated by MOLA (method 4) is similar to the result of method 2 and suggests that MOLA can be used for some smaller dunes. The barchanoid ridges (dunes 3 and 4) produced a wide range of measured heights. There was difficulty in applying the methods to these dunes (unclear slip face, sample location not at brink point etc.). Much of the variability in the data arises from the difficulty in fulfilling the specific requirements of each of the methods. We have annotated the results where measurement error could be readily estimated (see Table 1).

3.2. Transverse aeolian ridges (TARs)

In general, the three methods applied (1–3) are in good agreement for estimating bedform height. This is, in part, related to the quality of the data set for each of the methods, i.e., the high spatial resolution, good albedo conditions, and strong shadow definition. TAR heights range from 0.25 to 7 m. Method 2 seems to have the best agreement with method 3 when an angle of 10° is assumed. This angle is similar to terrestrial mega-ripple data (Williams et al., 2002) and might suggest that some TARs on Mars are mega-ripples rather than dunes.

4. Evaluation of methods

4.1. Method 1, stereography

This method is limited by restrictions on image geometry. More than 175,000 MOC narrow-angle images are released; but only a small subset of those overlap, and of those, even a smaller subset contain dunes. The requirement of overlapping MOC images therefore limits areas where stereography can be applied. A further limitation is that the overlapping images must have emission angles with enough angular separation to act as good stereo pairs.

Because stereography uses features such as boulders and outcrops to get a topographic section over an area larger than the dune alone, MOC images with the best resolutions possible should be used. Images with poorer resolution will introduce more error into the measurement of dune height. Finally, the dune and TAR brinks must be as parallel as possible to the MOC look direction in order to measure their heights. These limitations decrease the number of areas on Mars where dunes can be measured with stereography; but when requirements are met, this method will give reliable measurements. As MOC continues to collect images and other missions begin operations on Mars, stereography will become more widely used as a method for measuring heights of aeolian features.

4.2. Method 2, slip face length

The first key assumption (and therefore limitation) of this method is that the slip face is at the angle of repose of 33°. This is not always the case: Dunes that are no longer active tend to have lower lee slopes (e.g., Goudie et al., 1993). The potential scale of this type of error is illustrated in the results for the barchanoid ridges (dunes 3 and 4, Fig. 1D). A visual assessment of the slip face indicates that the lower lee slope is at a shallower angle than that of the upper. The result in this case is an overestimation of the height, perhaps by as much as 300%. Second, for estimations of maximum height, we assume that the brink represents the highest point of dune. This may not always be a valid assumption as the dune crest can be located farther toward the windward slope. However, on Earth, the dune brink and crest tend to merge in larger dunes, i.e. 100–500 m long (Embabi and Ashour, 1993), a scale similar to the dunes sampled in this study.

The advantage of this method is that it can be applied to the slip face of all dunes and estimates are calculated relatively rapidly, permitting morphometric measurements to be made on a large number of dunes. Another advantage is that an extended methodology has been developed whereby the measurement of several profiles on a dune can be used to construct an XY and Z grid at MOC scale for isolated dunes. These data can then be used to estimate the sediment volume of sand dunes on Mars (Bourke et al., 2004a).

4.3. Method 3, photoclinometry

For dune height measurements using this method, we found two limitations. First, it is necessary for the albedo of the dune material to be consistent with the surrounding terrain. This is found in locations of significant dust cover, or where interdune areas are sandy, and during seasonal frost cover. In this comparative methodological study, it is difficult to match these requirements with the same MOC images needed for analysis by method 1. Thus, some of the results are unreliable (see Table 1). By way of example, a profile was extracted from the same dune in two different images (dune 5 in FHA00451 and E0302016,

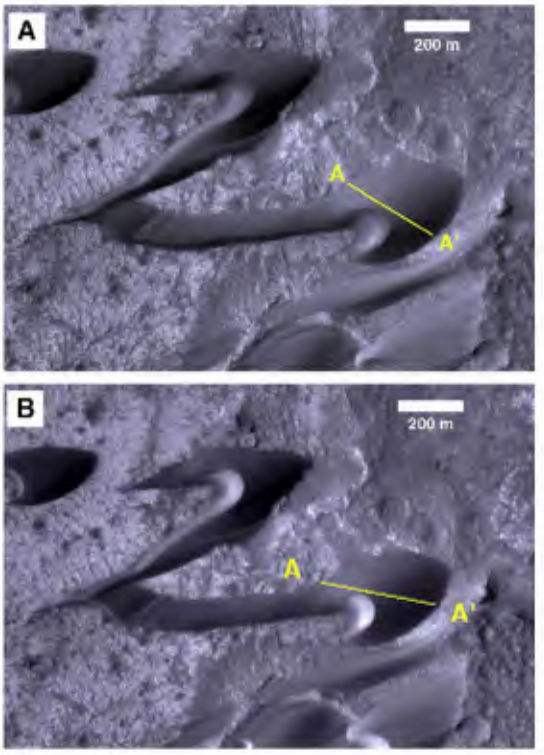

Fig. 3. Dune 5 located in a Syrtis Major caldera, 292.93° W., 8.88° N., (A) FHA-00451 2.95 m/px; image taken 1999-03-09. (B) E0302016 3.22 m/px; image taken 2001-04-24. Using method 3, a 30-m difference in the dune height was measured between these two images of the same dune. This is due to inherent errors in the method rather than a change in the dune over the 2-yr period.

Fig. 3). The resultant dune height estimates were 100 and 70 m respectively. The albedo data indicated that the latter height value was the more accurate. Dune transects were also placed so as to avoid frost patch or albedo changes (e.g. dunes 1, 3, 5; Fig. 1A, D, G) and as a result the profile does not always cross the highest part of the dune (e.g., Fig. 3).

Second, the location of the photoclinometry profile is dependent on the Sun azimuth relative to the dune alignment. The profile must also be in the down-Sun direction. This confining direction limits the application of this profiling photoclinometry technique to measuring topographic profiles in only one direction on any given image. If the landform of interest is not oriented appropriately with respect to the Sun in the scene, then measuring the topography is difficult. Axisymmetric features, like craters or circular hills, are the most robust to this constraint. Features with a linear orientation (such as transverse dunes) can be more difficult, but a correction can be made for this difference in slope azimuth.

The errors are cumulative in the creation of a topographic profile. The error in the elevation across the first pixel depends on the error in the distance across that first pixel, D, and the error in the slope, θ, for that pixel. However, the error in the elevation after the second pixel is dependent on the errors in D and θ for the second pixel as well as those in the first, and so on. So in addition to the difficulties of haze compensation, albedo variation, and slope azimuth (which contribute to the errors of the point photoclinometry technique), there is the added contribution of this cumulative error for the profiling photoclinometry technique. As a result, the absolute elevation difference between the beginning and end of a profile is not very reliable, and thus photoclinometric profiles should not be excessively long. However, relative elevation differences are reasonably reliable if they are separated by only a few tens of pixel distances.

An important advantage of this method is that it generates profile data for even the smallest scale dunes visible in the MOC images (Fig. 4). This will help determine whether scale-dependent trends, such as the steepening of windward slopes or the convergence of dune crest and brink that are found on terrestrial barchans (e.g., Embabi and Ashour, 1993), also occur on Martian dunes. In addition, the cross profiles of TARs (Fig. 4) can be compared to the growing data set on Earth mega-ripples (e.g., Lancaster et al., 2002; Williams et al., 2002; Wilson et al., 2003; Wilson and Zimbelman, 2004). Another distinct advantage of method 3 is the potential to estimate the height of dunes that do not have a well-developed or obvious slip face (e.g., domes or whalebacks; see dune 12, Fig. 1C).

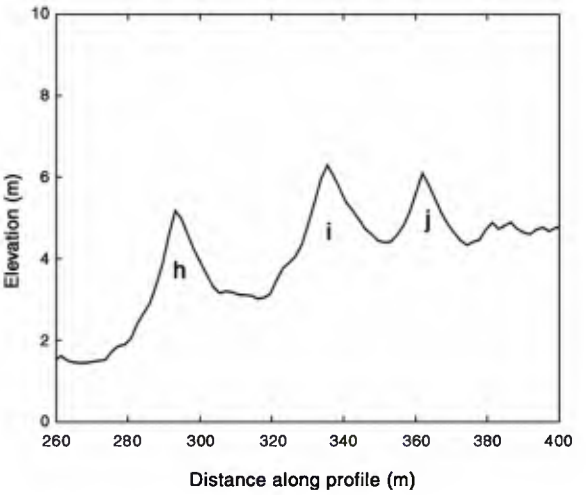

Fig. 4. Topographic profile generated by method 3 for TAR sample site D (for location see Fig. 2C). Slope angle, slope form, and wavelength can now be more precisely estimated for dunes on Mars.

4.4. Method 4, MOLA

The main limitations of this method are the accuracy of MOLA footprint position (dictated by the accuracy of MOLA alignment with MOC images) and the size of the MOLA footprint. The radial accuracy of individual profiles is ~1 m root mean square, and shot locations are determined to within 100 m in the along-track and across-track directions (Slavney and Neumann, 2003). Shan et al. (2002) found that MOC images can be registered to a MOLA profile at a precision of ~1–2 MOLA footprint spacing (i.e., 300–600 m). These errors are reduced considerably when the two data sets (MOC and MOLA) are acquired simultaneously, and the center of a MOLA shot can be registered to a specific pixel. This was determined for our sample sites by assessment of the co-registered data available at the PDS imaging node (http://pdsimg.jpl.nasa.gov/). Second, even where MOLA footprints coincide with the dune crest they represent an average height collected over a sloping surface (often ~33° on the lee slope and ~15° on the windward slope). These combined errors suggest that the approach should be limited to the larger dunes and dune masses.

4.5. Empirical estimates

There are constraints when estimating dune height on Mars using empirical estimates developed for Earth dunes. First, it is uncertain whether, under the very different atmospheric and gravity conditions, that dunes would adjust their morphometry in a similar way. Second, simple barchan dunes on Mars are, on average, larger than those on Earth. Bourke et al. (2004a) found that the mean width of barchans in the North Polar Sand Sea and the inter-crater dune fields were 290 and 430 m respectively. On Earth, the average width of barchans is smaller (e.g., 37 m wide in southern Peru (Finkel, 1959); 108 m wide in the Salton Sea, (Long and Sharp, 1964); 153.5 m wide in the Kharga Depression, Egypt (Stokes et al., 1999)). Hesp and Hastings (1998) note that a larger range in dune width may occur for larger and higher barchan dunes. Therefore, the empirical estimates may not be appropriate for Martian barchans. Third, barchan dunes on Earth used in the empirical studies were (mostly) typically-shaped barchans. Only two of the dunes in this study approximate typically-shaped barchans (dunes 9 and 11). Other dunes are either 'ovoid' (where the ratio of the windward slope length to barchan horn-to-horn width is ~2.4; dunes 6 and 8). Dune 12, is a dome dune and the remainder of the 'barchan' dunes either display 'deflected asymmetry' (where deflection of the extended arm is lateral and increases the horn-to-horn width; dunes 1 and 2) or have considerable limb asymmetry/extension (dunes 5, 7, 10 and 14). The remaining dunes are barchanoid ridges and are not suitable for this method (dunes 3, 4, 13, 15, 16). Interestingly, five of our sample dunes show good agreement between method 2 and the empirical estimate of Hesp and Hastings (formulae 1) (1998) (i.e., fall within a ratio of 0.7–1.3). The estimates for the true barchan shaped dunes in the data set (dunes, 9 and 11) are similar to the height estimates by empirical methods (Table 3). It is reasonable to tentatively propose here that the relationship between dune morphometric parameters may be allometric on Mars. This is the subject of an ongoing study (Bourke et al., 2004a, in preparation). The data also suggest that the approach for estimating dune height by the four methods presented (with suitable methodological constraints), produce reasonable estimates.

5. Conclusion

The methods presented here provide data on a range of morphometric parameters, some of which were not previously available for dunes on Mars. These parameters include dune height, width, length, surface area, volume, and longitudinal and cross profiles. These data will facilitate a more accurate analysis of aeolian dunes on Mars. The relative strengths and weakness of these methods are summarized in Table 4.

The results of the comparative analysis of methods 1, 2, and 3 indicate that they are reasonable approaches for estimating TAR height. Methods 1, 2 and (potentially) 4 give acceptable estimates for barchans, if the specific requirements for each method are strictly adhered to. Method 3 has great potential, but the selected barchans were not ideally suited for this method. Method 1 is intrinsically the most powerful as it makes the fewest assumptions (e.g., no assumption of slip face angle or albedo) but relies on coverage of multiple images of the target area. Although the highest resolution data (MOC) available at present contain relatively few instances of stereo-coverage, increasing amounts of data release, at meter and centimeter-scale resolution, in the next few years will make this method more viable (e.g., the Mars Reconnaissance Orbiter, High Resolution Imager, super resolution channel). In the meantime, method 2 with its simple approach is most suited to multiple

Table 4
Summary table of advantages and limitations of each technique for dune morphometric analysis

Method	Advantages	Limitations
1. Stereography	—Generates topographic profiles.	—Relies on multiple coverage of target area so few targets are available.
	—Purely geometric technique with few assumptions made.	—Assumes that dune forms have not moved in time periods between image acquisitions.
	—Potential target areas increasing in number as more images are returned by spacecraft.	—Computationally complex.
2. Slip face measurements	—Measurements very quick and easy to perform.	—Uses assumed slip face angle. —Only single point measurements can be made, rather than profiles. —Cannot be used on dune forms without obvious slip faces.
3. Photoclinometry	—Generates topographic profiles with single-pixel spatial resolution, thus usable on even very small dunes.	—Albedo must be constant (or is assumed to be constant) over the measurement area.
	—Can be used for dune forms without obvious slip faces	—Position of topographic profiles dependent on Sun azimuth. —Computationally complex.
4. MOLA	—Uses well-calibrated data.	—Spatial resolution is poor so only suitable for the largest dune forms.
	—Purely geometric technique with very few assumptions. —Measurements easy to obtain.	—Heights averaged over entire footprint so even large dune forms might not be measured accurately at brink.

measurements and statistical studies of dune height and volume on Mars.

The application of these techniques are not restricted to aeolian dune forms. Other smaller landforms such as pingos, cinder cones, small channels and bars and small craters can also be measured by methods 1 and 3 and 4 (if suitable). However similar constraints and limitations, as outlined above, will apply to all small-scale landforms on Mars.

Initiatives at the USGS are improving the potential spatial resolution of elevation data using a combination of stereographic and photogrametric techniques (Soderblom and Kirk, 2003). Although not yet applied to aeolian landscapes, the method was used to produce high-resolution digital elevation models (DEM) to assess the safety of candidate landing sites for the Mars Exploration Rovers (Kirk et al., 2003). These models yielded ~ 10 m horizontal resolution and meter-scale vertical precision with slope errors of 1–3°. These DEMs are controlled to and consistent with the MOLA global data set at the limits of resolution. Another potential source of morphometric data may come from the High Resolution Stereo Camera (HRSC) instrument onboard the Mars Express spacecraft. These data are currently being used to produce (DEMs of Mars with resolution of ~300 m/pixel (Oberst et al., 2004). While these data will not be a great improvement on MOLA profiles, work is underway to create 50-m/pixel DEMs from HRSC. These latter data will be useful in determining heights and volumes of large dune masses on Mars.

Acknowledgements

This work resulted from NASA funded projects: MDAP NNG04GJ92G (MB), MDAP NAG5-513327 (KW), MDAP NAG5-11075 (JZ). The Malin Space Science Systems are thanked for provision of the MOC data http://www.msss.com/moc_gallery/. This is contribution 379 from PSI.

References

Anderson, F.S., Greeley, R., Xu, P., Lo, E., Blumberg, D.G., Haberle, R.M., Murphy, J.R., 1999. Assessing the Martian surface distribution of aeolian sand using a Mars general circulation model. Journal of Geophysical Research (Planets) 104 (E8), 18991–19002.

Arthur, D.W.G., 1979. Mars relative altitudes from shadows. Lunar and Planetary Science Conference. Lunar and Planetary Institute, Houston, Texas, pp. 47–48.

Bagnold, R.A., 1941. The Physics of Blown Sand and Desert Dunes. Methuen, London. 265 pp.

Bandfield, J.L., Hamilton, V.E., Christensen, P.R., 2000. A global view of Martian surface compositions from MGS-TES. Science 287, 1626–1630.

Beyer, R.A., McEwen, A.S., Kirk, R.L., 2003. Meter-scale slopes of candidate MER landing sites from point photoclinometry. Journal of Geophysical Research (Planets) 108 (E12). doi:10.1029/2003JE002120.

Bourke, M.C., Wilson, S.A., Zimbelman, J.R., 2003. The variability of transverse aeolian ridges in troughs on Mars. Lunar and Planetary Science conference. Lunar and Planetary Institute, Houston, Texas, p. 2090. Available at http://www.lpi.usra.edu/meetings/lpsc2003/pdf/2090.pdf.

Bourke, M.C., Balme, M., Zimbelman, J.R., 2004a. A comparative analysis of barchan dunes in the intra-crater dune fields and the north polar sand sea. Lunar and Planetary Science Conference. Lunar and Planetary Institute, Houston, Texas, p. 1453. Available at http://www.lpi.usra.edu/meetings/lpsc2004/pdf/1453.pdf.

Bourke, M.C., Bullard, J., Barnouin-Jha, O., 2004b. Aeolian sediment transport pathways and aerodynamics at troughs on Mars. Journal of Geophysical Research (Planets) 109 (E7). doi:10.1029/2003JE002155.

Bourke, M.C., Balme, M., Zimbelman, J.R., in preparation. A comparative morphometric analysis of isolated crescentic dunes in the North polar Sand Sea and Intra-crater dunefields.

Byme, S., Murray, B.C., 2002. North polar stratigraphy and the paleo-erg of Mars. Journal of Geophysical Research (Planets) 107 (E6). doi:10.1029/2001JE001615.

Christensen, P.R., Morris, R.V., Lane, M.D., Bandfield, J.L., Malin, M.C., 2001. Global mapping of Martian hematite mineral deposits: Remnants of water-driven processes on early Mars. Journal of Geophysical Research (Planets) 106 (E10), 23873–23885.

Christensen, P.R., McSween, H.Y., Bandfield, J.L., Ruff, S.W., Rogers, A.D., Hamilton, V.E., Gorelick, N., Wyatt, M.B., Jakosky, B.M., Kieffer, H.H., Malin, M.C., Moersch, J.E., 2005. Evidence for magmatic evolution and diversity on Mars from infrared observations. Nature 436 (7050), 504–509.

Edgett, K.S., 2002. Low albedo surfaces and eolian sediment: Mars Orbiter Camera views of Westem Arabia Terra craters and wind streaks. Journal of Geophysical Research (Planets) 107 (E6). doi:10.1029/2001JE001587.

Edgett, K., Christensen, P.R., 1991. The particle size of Martian aeolian dunes. Journal of Geophysical Research (Planets) 96 (E5), 22,765–22,776.

Edgett, K.S., Malin, M.C., Sullivan, R.J., Thomas, P., Veverka, J., 2000. Dynamic Mars: New dark slope streaks observed on annual and decadal time scales. Lunar and Planetary Science Conference. Lunar and Planetary Institute, Houston, Texas, p. 1058.

Edgett, K.S., Williams, R.M.E., Malin, M.C., Cantor, B.A., Thomas, P.C., 2003. Mars landscape evolution: influence of stratigraphy on geomorphology in the north polar region. Geomorphology 52 (3–4), 289–297.

Embabi, N.S., Ashour, M.M., 1993. Barchan dunes in Qatar. Journal of Arid Environments 25 (1), 49–69.

Ewing, R.C., 2004. Pattern variability in natural dune fields. MS Thesis, University of Texas, Austin. 113 pp.

Fenton, L.K., Richardson, M.I., 2001. Martian surface winds: Insensitivity to orbital changes and implications for aeolian processes. Journal of Geophysical Research (Planets) 106, 32885–32902.

Fenton, L.K., Bandfield, J.L., Ward, A.W., Wesley, A., 2003. Aeolian processes in Proctor Crater on Mars: sedimentary history as analyzed from multiple data sets. Journal of Geophysical Research (Planets) 108 (E12). doi:10.1029/2002JE002015.

Fenton, L.K., Toigo, A.D., Richardson, M.I., 2005. Aeolian processes in Proctor Crater on Mars: mesoscale modeling of dune-forming winds. Journal of Geophysical Research (Planets) 110 (6), 1–18.

Finkel, H.J., 1959. The barchans of southem Peru. Journal of Geology 67, 614–647.

Fishbaugh, K.E., Head, J.W., 2005. Origin and characteristics of the Mars north polar basal unit and implications for polar geologic history. Icarus 174 (2), 444–474.

Garvin, J.B., Frawley, J.J., Sakimoto, S.E.H., 1999. North polar dunes on Mars: MOLA measurements and implications for sediment volumes. Lunar and Planetary Science Conference. Lunar and Planetary Institute, Houston, Texas, p. 1721. Available at http://www.lpi.usra.edu/meetings/LPSC99/pdf/1721.pdf.

Goudie, A.S., Stokes, S., Livingstone, I., Bailiff, I.K., Allison, R.J., 1993. Post-depositional modification of the linear sand ridges of the West Kimberley area of north-west Australia. The Geographical Journal 159 (3), 306–317.

Greeley, R., Kraft, M., Sullivan, R., Wilson, G., Bridges, N., Herkenhoff, K., Kuzmin, R.O., Malin, M., Ward, W., 1999. Aeolian features and processes at the Mars Pathfinder landing site. Journal of Geophysical Research (Planets) 104 (E4), 8573–8584.

Greeley, R., Bridges, N.T., Kuzmin, R.O., Laity, J.E., 2002. Terrestrial analogs to wind-related features at the Viking and Pathfinder landing sites on Mars. Journal of Geophysical Research (Planets) 107 (E12).

Greeley, R., Squyres, S.W., Arvidson, R.E., Bartlett, P., Bell III, J.F., Blaney, D., Cabrol, N.A., Farmer, J., Farrand, B., Golombek, M.P., Gorevan, S.P., Grant, J.A., Haldemann, A.F.C., Herkenhoff, K.E., Johnson, J., Landis, G., Madsen, M.B., McLennan, S.M., Moersch, J., Rice Jr., J.W., Richter, L., Ruff, S., Sullivan, R.J., Thompson, S.D., Wang, A., Weitz, C.M., Whelley, P., 2004. Wind-Related Processes Detected by the Spirit Rover at Gusev Crater, Mars. Science 305 (5685), 810–813.

Haberle, R.M., Joshi, M.M., Murphy, J.R., Barnes, J.R., Schofield, J. T., Wilson, G., Lopez-Valverde, M., Hollingsworth, J.L., Bridger, A.F.C., Schaeffer, J., 1999. General circulation model simulations of the Mars Pathfinder atmospheric structure investigation/meteorology data. Journal of Geophysical Research (Planets) 104 (E4), 8957–8974.

Hastenrath, S.L., 1967. The barchans of the Arequipa region, southern Peru. Zeitschrift fur Geomorphologie 11, 300–311.

Hastenrath, S.L., 1987. The barchan dunes of southem Peru revisited. Zeitschrift fur Geomorphologie 31, 167–178.

Hayward, R.K., Mullins, K.F., Hare, T.M., Titus, T.N., Fenton, L.K., Bourke, M., Colprete, A., Christensen, P.R., 2004. Mars Digital Dune Database. Eos Transactions Fall Meetting 85 (46) 31B-0984.

Hesp, P.A., Hastings, K., 1998. Width, height and slope relationships and aerodynamic maintenance of barchans. Geomorphology 22 (2), 193–204.

Howard, A.D., Blasius, K.R., Cutts, J.A., 1982. Photoclinometric determination of the topography of the Martian north polar cap. Icarus 50 (2–3), 245–258.

Jaumann, R., Reiss, D., Frei, S., Scholten, F., Gwinner, K., Roatsch, T., Matz, K.-D., Mertens, V., Hauber, E., Hoffmann, H., Köhler, U., Neukum, G., Head, J.W., Hiesinger, H., Carr, M.H., 2005. Interior channels in Martian valleys: constraints on fluvial erosion by measurements of the Mars Express High Resolution Stereo Camera. Geophysical Research Letters 32 (16), 1–4.

Kirk, R.L., Howington-Kraus, E., Redding, B., Galuszka, D., Hare, T. M., Archinal, B.A., Soderblom, L.A., Barrett, J.M., 2003. High-resolution topomapping of candidate MER landing sites with Mars Orbiter Camera narrow-angle images. Journal of Geophysical Research (Planets) 108. doi:10.1029/2003JE002131.

Lancaster, N., 1988. Controls of eolian dune size and spacing. Geology 16, 972–975.

Lancaster, N., Nickling, W.G., Gillies, J.A., 2002. Exceptionally coarse-grained wind ripples in the Wright Valley, Antarctica. In: Lee, J.A., Zobeck, T.M. (Eds.), Proceedings of ICAR5/GCTE-SEN Joint Conference. International Center for Arid and Semiarid

Lands Studies, Texas Tech University. Available at http://www.csrl.ars.usda.gov/wewc/icar5/.

Langevin, Y., Poulet, F., Bibring, J.-P., Gondet, B., 2005. Sulfates in the north polar region of Mars detected by OMEGA/Mars Express. Science 307 (5715), 1584–1586.

Long, J.T., Sharp, R.P., 1964. Barchan-dune movement in Imperial Valley, California. Geological Society of America Bulletin 75, 149–156.

Mabbutt, J.A., 1977. Desert Landforms. Australian National University Press, Canberra. 340 pp.

Malin, M.C., Edgett, K.S., 2001. The Mars global surveyor Mars orbiter camera: interplanetary cruise through primary mission. Journal of Geophysical Research (Planets) 106 (E10), 23,429–23,570.

Miyamoto, H., Dohm, J.M., Baker, V.R., Beyer, R.A., Bourke, M., 2004. Dynamics of unusual debris flows on Martian sand dunes. Geophysical Research Letters 31. doi:10.1029/2004GL020313.

Mullins, K.F., Hayward, R.K., Bourke, M., Titus, T.N., Fenton, L.K., Christensen, P.R., 2004. Areal estimates of dune deposits in Kaiser Crater on Mars. Eos Transactions Fall Meeting 85 (46), P21B-03.

Nagihara, S., Mulligan, K.R., Xiong, W., 2004. Use of a three-dimensional laser scanner to digitally capture the topography of sand dunes in high spatial resolution. Earth Surface Processes and Landforms 29, 391–398.

Neumann, G.A., 2003. Polar dunes resolved by the Mars Orbiter Laser Altimeter gridded topography and pulse widths. Sixth International Conference on Mars. Lunar and Planetary Institute, Pasadena, California, p. 3262. Available at http://www.lpi.usra.edu/meetings/sixthmars2003/pdf/3262.pdf.

Oberst, J., Roatsch, T., Giese, B., Wählisch, M., Scholten, F., Gwinner, K., Matz, K.-D., Hauber, E., Neukum, G., Jaumann, R., Ebner, H., Spiegel, M., vanGasselt, S., Albertz, J., Gehrke, S., Heipke, C., Schmidt, R., 2004. The mapping performance of The HRSC / SRC In Mars orbit, IAPRS, vol. XXXV, available at http://www.isprs.org/istanbul2004/comm4/papers/546.pdf, Istanbul, pp. 1318–1323.

Parker, T.J., Schenk, P.M., 1995. Viking Stereo of the Martian crustal dichotomy in southern Elysium: evidence for extensive fluvial and coastal erosion? Lunar and Planetary Science Conference. Lunar and Planetary Institute, Houston, Texas, p. 1105.

Pye, K., Tsoar, H., 1990. Aeolian Sand and Sand Dunes. Unwin Hyman, London. 396 pp.

Rafkin, S.C.R., Michaels, T.I., 2003. Meteorological predictions for 2003 Mars Exploration Rover high-priority landing sites. Journal of Geophysical Research (Planets) 108 (E12). doi:10.1029/2002JE002027.

RoverTeam, 1997. Characterization of the Martian surface deposits by the Mars Pathfinder Rover, Sojourner. Science 278, 1765–1767.

Shan, J., Lee, D.S., Yoon, J.S., 2002. Photogrammetric registration of MOC imagery to MOLA profile. Symposium on Geospatial Theory. Processes and Applications, Ottawa, Canada.

Sharp, R.P., 1963. Wind ripples. Journal of Geology 71, 617–636.

Slavney, S., Neumann, G., 2003. Instrument Information: Mars Orbiter Laser Altimeter http://wwwpds.wustl.edu/missions/mgs/catalog/inst_mola.txt.

Smith, D.E., Zuber, M.T., Frey, H.V., Garvin, J.B., Head, J.W., Muhleman, D.O., Pettengill, G.H., Phillips, R.J., Solomon, S.C., Zwally, H.J., Banerdt, W.B., Duxbury, T.C., 1998. Topography of the Northern Hemisphere of Mars from the Mars Orbiter Laser Altimeter. Science 279, 1686.

Smith, D.E., Zuber, M.T., Solomon, S.C., Phillips, R.J., Head, J.W., Garvin, J.B., Banerdt, W.B., Muhleman, D.O., Pettengill, G.H., Neumann, G.A., Lemoine, F.G., Abshire, J.B., Aharonson, O., Brown, C.D., Hauck, S.A., Ivanov, A.B., McGovern, P.J., Zwally, H.J., Duxbury, T.C., 1999. The global topography of Mars and implications for surface evolution. Science 284, 1495.

Smith, D.E., Zuber, M.T., Frey, H.V., Garvin, J.B., Head, J.W., Muhleman, D.O., Pettengill, G.H., Phillips, R.J., Solomon, S.C., Zwally, H.J., Banerdt, W.B., Duxbury, T.C., Golombek, M.P., Lemoine, F.G., Neumann, G.A., Rowlands, D.D., Aharonson, O., Ford, P.G., Ivanov, A.B., Johnson, C.L., J., M.P.,, Abshire, J.B., Afzal, R.S., Sun, X., 2001. Mars Orbiter Laser Altimeter: experiment summary after the first year of global mapping of Mars. Journal of Geophysical Research (Planets) 106 (E10), 23689–23722.

Soderblom, L.A., Kirk, R.L., 2003. Meter-scale 3-D models of the Martian surface from combining MOC and MOLA data. Lunar and Planetary Institute Conference. Lunar and Planetary Institute, Houston, Texas, p. 1730. available at http://www.lpi.usra.edu/meetings/lpsc2003/pdf/1730.pdf.

Stokes, S., Goudie, A.S., Ballard, J., Gifford, C., Samieh, S., Embabi, N., El-Rashidi, O.A., 1999. Accurate dune displacement and morphometric data using kinematic GPS. Zeitschrift fur Geomorphologie 116, 195–214.

Sullivan, R.J., Bell III, J.F., Calvin, W.M., Fike, D., Golombek, M.P., Greeley, R., Grotzinger, J.P., Herkenhoff, K.E., Jerolmack, D., Malin, M.C., Ming, D., Soderblom, L.A., Squyres, S.W., Thompson, S., Watters, W.A., Weitz, C.M., Yen, A.S., 2005. Aeolian processes at the Mars exploration rover opportunity landing site. Lunar and Planetary Science Conference. Lunar and Planetary Institute, Houston, Texas, p. 1942. Available at http://www.lpi.usra.edu/meetings/lpsc2005/pdf/1942.pdf.

Thomas, P., Weitz, C., 1989. Sand dunes and polar layered deposits on Mars. Icarus 81, 185–215.

Toigo, A.D., Richardson, M.I., 2003. Meteorology of proposed Mars Exploration Rover landing sites. Journal of Geophysical Research (Planets) 108l. doi:10.1029/2003JE002064.

Whalley, W.B., 1990. Physical Properties. In: Goudie, A.S. (Ed.), Geomorphological Techniques. Unwin Hyman, London, p. 570.

Williams, K.K., 2003. Measurements of dune heights on Mars. Sixth International Conference on Mars. Lunar and Planetary Institute, Pasedena, p. 3220. Available at http://www.lpi.usra.edu/meetings/sixthmars2003/pdf/3220.pdf.

Williams, K.K., Greeley, R., Zimbelman, J.R., 2003. Using overlapping MOC images to search for dune movement and to measure dune heights. Lunar and Planetary Science Conference. Lunar and Planetary Institute, Houston, Texas, p. 1639. Available at http://www.lpi.usra.edu/meetings/lpsc2003/pdf/1639.pdf.

Williams, K.K., Zimbelman, J.R., 2003. First measurement of ripple heights on Mars. Geological Society of America Abstracts with Programs 35 (6), 167.

Williams, S.H., Zimbelman, J.R., Ward, A.W., 2002. Large ripples on Earth and Mars. Lunar and Planetary Science Conference. Lunar and Planetary Institute, Houston, Texas, p. 1508. Available at http://www.lpi.usra.edu/meetings/lpsc2002/pdf/1508.pdf.

Wilson, S.A., Zimbelman, J.R., 2004. Latitude-dependent nature and physical characteristics of transverse aeolian ridges on Mars. Journal of Geophysical Research (Planets) 109 (E10003). doi:10.1029/2004JE002247.

Wilson, S.A., Zimbelman, J.R., Williams, S.H., 2003. Large aeolian ripples: extrapolation from Earth to Mars. Lunar and Planetary Science Conference. Lunar and Planetary Institute, Houston, Texas, p. 1862. Available at http://www.lpi.usra.edu/meetings/lpsc2003/pdf/1862.pdf.

Wyatt, M.B., McSween, H.Y., 2002. Spectral evidence for weathered basalt as an alternative to andesite in the northern lowlands of Mars. Nature 417, 263–266.

Zimbelman, J.R., Leshin, L.A., 1987. A geologic evaluation of thermal properties for the Elysium and Aeolis quadrangles of Mars. Journal of Geophysical Research (Planets) 92 (B4), 588–596.

Zimbelman, J.R., 2000. Non-active dunes in the Acheron Fossae region of Mars between the Viking and Mars Global Surveyor eras. Geophysical Research Letters 27 (7), 1069–1072.